[CANCER RESEARCH 61, 2736–2743, March 15, 2001]

Angiogenesis and Prostate Cancer: Identification of A Molecular Progression Switch[1]

Wendy J. Huss, Colleen F. Hanrahan, Roberto J. Barrios, Jonathan W. Simons, and Norman M. Greenberg[2]

Department of Molecular and Cellular Biology [W. J. H., N. M. G.], Scott Department of Urology [N. M. G.], and Department of Pathology [R. J. B.], Baylor College of Medicine, Houston, Texas 77030; The Johns Hopkins Oncology Center, Brady Urological Institute, The Johns Hopkins University School of Medicine, Baltimore, Maryland 21287 [C. F. H.]; and Winship Cancer Institute, Emory University School of Medicine, Atlanta, Georgia 30321 [J. W. S.]

ABSTRACT

To elucidate the sequence of molecular events intricate with angiogenesis and the initiation and progression prostate cancer, the temporal and spatial expression patterns of platelet endothelial cell adhesion molecule-1 (PECAM-1/CD31), hypoxia-induced factor-1 α (HIF-1α), vascular endothelial growth factor (VEGF), and the cognate receptors VEGFR1 and VEGFR2 were characterized. Immunohistochemical and *in situ* analyses of prostate tissue specimens derived from the spontaneous autochthonous transgenic adenocarcinoma of the mouse prostate (TRAMP) model identified a distinct early angiogenic switch consistent with the expression of PECAM-1, HIF-1α, and VEGFR1 and the recruitment of new vasculature to lesions representative of high-grade prostatic epithelial neoplasia (PIN). During progression of prostate cancer, the intraductal microvessel density (IMVD) was also observed to increase as a function of tumor grade. Immunoblot and *in situ* analyses further demonstrated a distinct late angiogenic switch consistent with decreased expression of VEGFR1, increased expression of VEGFR2, and the transition from a differentiated adenocarcinoma to a more poorly differentiated state. Analysis of clinical prostate cancer specimens validated the predictions of the TRAMP model. This resolution of prostate cancer-associated angiogenesis into distinct early and late molecular events establishes the basis for a "progression-switch" model to explain how the targets of antiangiogenic therapy might change as a function of tumor progression.

INTRODUCTION

The ability of a tumor to recruit new vasculature is requisite for growth beyond a small nodule (1). During this vascularization, a process termed angiogenesis, endothelial cells initially respond to changes in the local environment and migrate toward the growing tumor. The endothelial cells then migrate together forming tubular structures that are ultimately encapsulated by recruiting periendothelial support cells to establish a vascular network that facilitates tumor growth and metastasis (2). Although this schema for angiogenesis is generally accepted, the earliest molecular events that dictate the "angiogenic switch" remain elusive in a disease such as prostate cancer, probably because they occur before a clinical diagnosis can be definitively established.

Investigations into the molecular basis of tumor vascularization have previously demonstrated that tumors express a number of autocrine and paracrine factors that activate or otherwise facilitate this process. These include VEGF,[3] basic FGF (FGF-2), acidic FGF (FGF-1), matrix metalloproteinases, insulin-like growth factor I, and angiopoietin-1 (3). VEGF and the closely related proteins VEGF-B and VEGF-C are very potent proangiogenic factors that are expressed by several types of tumors (4–7). Expression of VEGF has been shown in prostate cells of normal, benign, and malignant phenotypes (8–10). For example, in a study of patients with either BPH or organ-confined prostate cancer, no statistically significant difference was observed in the levels of urinary VEGF between these groups and the normal controls (11). In the Dunning R3327 PAP tumor model VEGF, VEGFR1, and VEGFR2 mRNA levels were elevated compared with normal ventral prostate (12). However, VEGF was readily detected in the serum of mice harboring orthotopic grafts of the PC-3 M and DU145 prostate cancer cell lines (13). Although tumor cells may express VEGF, expression of the cognate receptors VEGFR1 and VEGFR2 is generally believed to be restricted to endothelial cells.

Identification of the molecular mechanisms regulating expression of VEGF, VEGFR1, and VEGFR2 is a subject of intense investigation. For example, hypoxic conditions have been demonstrated to regulate expression of VEGF, VEGFR1, and VEGFR2 (14). VEGF and VEGFR1 were both observed to be up-regulated by the transcription factor HIF-1α (15–17). Furthermore, a HIF-2α response element was identified in the regulatory region of the *VEGFR2* gene (18). A number of peptide and steroid hormones associated with prostate cancer growth such as basic FGF2, insulin-like growth factor I, and androgens have also been shown to regulate expression of VEGF (19–21).

The mechanism of VEGFR signal transduction is complex. Many signaling proteins have been shown to be associated with the activated VEGFR1, including: SHP-2, p27, Grb2, PLCγ, Crk, and NCK (22). However VEGFR1 does not appear to signal through the MAPK cascade or induce endothelial cell proliferation, yet it appears to be important in endothelial cell migration (23). On the other hand, VEGFR2 is believed to signal through both the MAPK cascade to induce endothelial cell proliferation as well as the PI3′K to activate an antiapoptotic pathway (24, 25).

Equally important to the activators of the angiogenic phenotype are the molecules that inhibit this process. In fact, it has been proposed that a tumor will become vascularized as a consequence of stochastic events that disrupt any balance that exists between the activators and inhibitors (2). Molecules that posses antiangiogenic properties, such as thrombospondin-1, IFN α/β, tissue inhibitor of metalloproteinase-1, angiopoietin-2, endostatin and angiostatin, are currently being isolated, characterized, and exploited as potential therapeutics (3). It is obvious that a better understanding of the temporal and spatial patterns of expression of molecules that regulate this process will be required to develop more effective diagnostics and therapeutics.

The complex nature of the VEGF signaling axis and the inherent interactions between epithelium, stroma, and endothelium have made the angiogenic switch difficult to characterize during the natural history of clinical prostate cancer. Hence, we have chosen to examine the molecular changes in the VEGF signaling axis in the autochthonous spontaneous TRAMP model. Briefly, TRAMP mice express a

Received 8/24/00; accepted 1/12/01.

The costs of publication of this article were defrayed in part by the payment of page charges. This article must therefore be hereby marked *advertisement* in accordance with 18 U.S.C. Section 1734 solely to indicate this fact.

[1] This study was supported by National Cancer Institute Grant CA64851 (to N. M. G.), Specialized Program of Research Excellence (SPORE) CA58204 (to N. M. G.), and an award from the Scott Department of Urology Prostate Cancer Research Initiative (to N. M. G. and W. J. H.).

[2] To whom requests for reprints should be addressed, at Department of Molecular and Cellular Biology, Baylor College of Medicine, One Baylor Plaza, M626A, Houston, TX 77030. Phone: (713) 798-3819; Fax: (713) 798-8012; E-mail: normang@bcm.tmc.edu.

[3] The abbreviations used are: VEGF, vascular endothelial growth factor; VEGFR, VEGF eceptor; FGF, fibroblast growth factor; BPH, benign prostatic hypertrophy; HIF, hypoxia-induced factor; MAPK, mitogen-activated protein kinase; PBS, phosphate-buffered saline; PI3′K, phosphotidyl inositol 3′ kinase; TBST, Tris-buffered saline with Tween; TRAMP, transgenic adenocarcinoma of the mouse prostate; PIN, prostatic intraepithelial neoplasia; PECAM, platelet endothelial cell adhesion molecule; IMVD, intraductal microvessel density; sVEGFR1, soluble form of VEGFR1.

PB-SV40 early gene (T/t antigen; Tag) construct under prostate specific control of the minimal rat probasin promoter and display mild to severe hyperplasia of the prostate epithelium, resembling PIN by 6–12 weeks of age (26). Well-differentiated neoplasia is generally observed in TRAMP mice between 10 and 16 weeks of age, and between 18 and 24 weeks of age, all of the mice will display primary tumors and metastases to distant sites (27, 28). The restricted temporal and spatial pattern of prostate cancer progression in TRAMP affords a unique window of opportunity for investigation of the earliest molecular events of the disease. By investigating angiogenesis in the TRAMP model, we now demonstrate that the angiogenic switch is, in fact, a series of sequential molecular events that resolve to a distinct early "initiation event" and a later "progression event." The initiation event corresponds to the expression of HIF-1α and VEGFR1, whereas the progression event corresponds to the expression of VEGFR2 and the transition from a differentiated adenocarcinoma to a more poorly differentiated state. Subsequent analysis of clinical prostate cancer specimens was used to confirm and validate the predictions of the TRAMP model. Taken together, these data establish the basis for a "progression-switch" model to explain how the targets of antiangiogenic therapy change as a function of tumor progression and to ascertain that VEGFR2 is a logical target for intervention therapy.

MATERIALS AND METHODS

Transgenic Mice. TRAMP mice, heterozygous for the *PB-Tag* transgene, were maintained in a C57BL/6 background (Harlan Sprague Dawley, Inc., Indianapolis IN; Ref. 26) and crossed with nontransgenic FVB mice to obtain transgenic and nontransgenic [C57BL/6 × FVB] F1 males. Isolation of tail DNA and PCR screening were performed as described previously (26). TRAMP mice and nontransgenic littermates were randomly assigned into cohorts and sacrificed at 6, 12, 18, and 24 weeks of age. In addition, a cohort of TRAMP mice were castrated by a scrotal approach at 12 weeks of age and sacrificed at 24 weeks of age. Of the castrated TRAMP mice that developed tumors, 20% did not develop carcinomas as determined at necropsy. Mice that did not show a durable response to castration were used as a source of prostate tumor tissue representing androgen-independent disease. Approximately one-half of each prostate specimen was used for histological analysis and subsequent pathological grading according to a previously described scheme (28). Remaining tissues were stored at −80°C and used for protein analysis. All of the experiments were conducted using the highest standards for humane care in accordance with the NIH Guide for the Care and Use of Laboratory Animals.

Clinical Prostate Samples. Prostate tissue was obtained from the S.P.O.R.E. prostate tissue bank at Baylor College of Medicine. The clinical specimens represented Gleason grades 5–7, and normal sections from each patient were used as controls.

Western Blot Analysis. Total cell lysates were prepared by tissue homogenization in RIPA buffer [50 mM Tris (pH 8.0), 1% Triton X-100, 150 mM NaCl, 0.02% sodium azide, 5 μg/ml leupeptin, 5 μg/ml pepstatin, 1 mM phenylmethanesulfonyl fluoride]. Approximately 40 μg of protein from each tumor sample was denatured in loading buffer [100 mM Tris (pH 6.8), 0.01% β-mercaptoethanol, 20% glycerol, 4% SDS] by boiling for 10 min and loaded onto a 7.5 or 12% SDS-polyacrylamide gel. Proteins were separated by electrophoresis and then transferred to Immobilon-P membrane (Millipore, Bedford, MA). The filters were blocked for 1 h in TBST [0.1 M Tris (pH 7.4), 1.5 N NaCl, 0.5% Tween 20], 5% nonfat dry milk, and 2% BSA. When appropriate, blots were incubated overnight at 4°C in 3% nonfat dry milk in TBST with a rabbit polyclonal antibody specific for VEGF diluted 1:400 (Ab-1; Neomarkers, Fremont, CA), or a rabbit polyclonal antibody specific for VEGFR1/Flt-1 diluted 1:100 (C-17; Santa Cruz, Santa Cruz, CA), or a rabbit polyclonal antibody VEGFR2/Flk-1 diluted 1:1000 (N-931; Santa Cruz), or a monoclonal antibody specific for β-Actin diluted 1:5000 (AC-74, Sigma). After several washes in 0.5% nonfat dry milk in TBST, filters were incubated with either horseradish peroxidase-conjugated α-rabbit or α-mouse (Amersham, Piscataway, NJ) IgG antibody diluted 1:5000 for 1 h at room temperature in 3% nonfat dry milk in TBST. After several washes with 0.5% nonfat dry milk the filters were developed with enhanced chemiluminescent (ECL) detection system (Pierce, Rockford, IL) according to the manufacturer's recommended protocol and exposed to X-Ray film (XAR-1; Eastman Kodak, Rochester, NY). The Western analysis was scored as either positive for a band present at the appropriate size or negative when there was no evidence of a band at the appropriate size; all of the blots were performed in duplicate, and each contained at least one positive and one negative sample.

Immunohistochemistry. Tissues procured at necropsy were fixed in 4% paraformaldehyde for 4 h and then transferred to 70% ethanol and embedded in paraffin, and 5-μm sections were cut and mounted on ProbeOn-Plus slides (Fisher, Houston TX). Slides were hydrated through xylene and graded alcohol and equilibrated in PBS. Antigen retrieval was performed with 10 μg/ml proteinase K (Amresco, Solon, OH) at 37°C for 10 min. Endogenous peroxidases were quenched with 3% H_2O_2 in methanol. Nonspecific binding was blocked with Power Block (BioGenex, San Ramon, CA) according to manufacturer's recommendations. When appropriate, slides were incubated with a rat monoclonal antibody specific for CD31/PECAM-1 (PharMingen, San Diego, CA) at a 1:50 dilution. Immunodetection of HIF-1α was performed essentially as described previously (29). All of the slides were subsequently washed several times in PBS with 0.1% Tween 20 and were incubated with a 1:100 dilution of biotin-conjugated goat antirat IgG (PharMingen, San Diego, CA) or 1:2000 dilution of biotin-conjugated goat antirabbit IgG (Vector Laboratories, Burlingame, CA) for 1 h at room temperature. Immunoreactive species were detected with the Vectastain Elite ABC immunoperoxidase system according to the manufacturer's recommendations, (Vector Laboratories, Burlingame, CA). Sections were counterstained with methyl green, dehydrated through graded alcohol into xylene, and mounted under glass coverslips.

IMVD. To determine IMVD, sections were stained with an antibody to CD31/PECAM-1 as described above. The number of intraductal vessels was determined by counting three high-power (×40) fields of the highest vascular density. The averaged IMVD for each specimen was determined and statistical analysis was performed by nonparametric ANOVA multiple comparisons with tumor grade using Fisher's least significant difference. Interductal vessels were considered to be normal vasculature.

Mouse VEGF Immunoassay. The Quantikine M Mouse VEGF immunoassay (R&D Systems, Minneapolis, MN) was used to determine serum levels of VEGF according to the manufacturer's recommendations. Briefly, blood samples collected from TRAMP mice and nontransgenic littermates prior to sacrifice were allowed to clot for several hours and serum fraction was recovered after centrifugation. Serum was stored at −20°C. All of the sera were diluted 5-fold in supplied diluent, and the immunoassay was performed with supplied standards and controls. Statistical analysis was performed using nonparametric ANOVA multiple comparisons.

***In Situ* Hybridization.** To detect the VEGF axis by *in situ* hybridization, ^{33}P-antisense and -sense RNA probes were synthesized from linearized plasmids containing subcloned cDNA fragments. To generate the probes total RNA was first isolated from 12-day mouse embryos using Trizol (Life Technologies, Grand Island, NY) according to the manufacturer's recommendations. All of the probes were then generated by reverse transcription-PCR using 1 μg of total RNA as template essentially as described previously (30). The VEGF probe (213-bp), pVEGF-213, was prepared with primers that amplified within exons 1–5 that are shared between all splice forms (forward, 5′-ATGGACGTCTACCAGCGAAG; and reverse, 5′-GCTTTGGTGAGGTTTGATCC), corresponding to bp 213–426 of GenBank accession number M95200 (31). The VEGF-B-probe (215 bp), pVEGF-B-215, was amplified with primers (forward, 5′-CCAGAAGAAAGTGGTGCCAT; and reverse, 5′-ATGAGGATCTGCATTCGGAC) corresponding to bp 285–500 of GenBank accession number MMU43836 (32). The VEGF-C-probe (290 bp), pVEGF-C-290, was amplified with primers (forward, 5′-TGTGTCCAGCGTAGATGAGC; and reverse, 5′-CCACATCTGTAGACGGACAC) corresponding to bp 339–629 of GenBank accession number U73620 (33). The sVEGFR1/sFlt-1 probe (316 bp), psVEGFR1–316, was amplified with primers (forward, 5′-AAATTTAAAAGCAGGAGGATT; and reverse, 5′-TTGCTGCTATGAAGCAGAAGA) corresponding to bp 2265–2581 of GenBank accession number D88690 (34). The VEGFR1/Flt-1 probe (268 bp), pVEGFR1–268, was amplified with primers (forward, 5′-AACAGCACGCTGTTTATTGAA; and reverse, 5′-ATCTGGGTCCATAATGATTGA) corresponding to bp 2166–

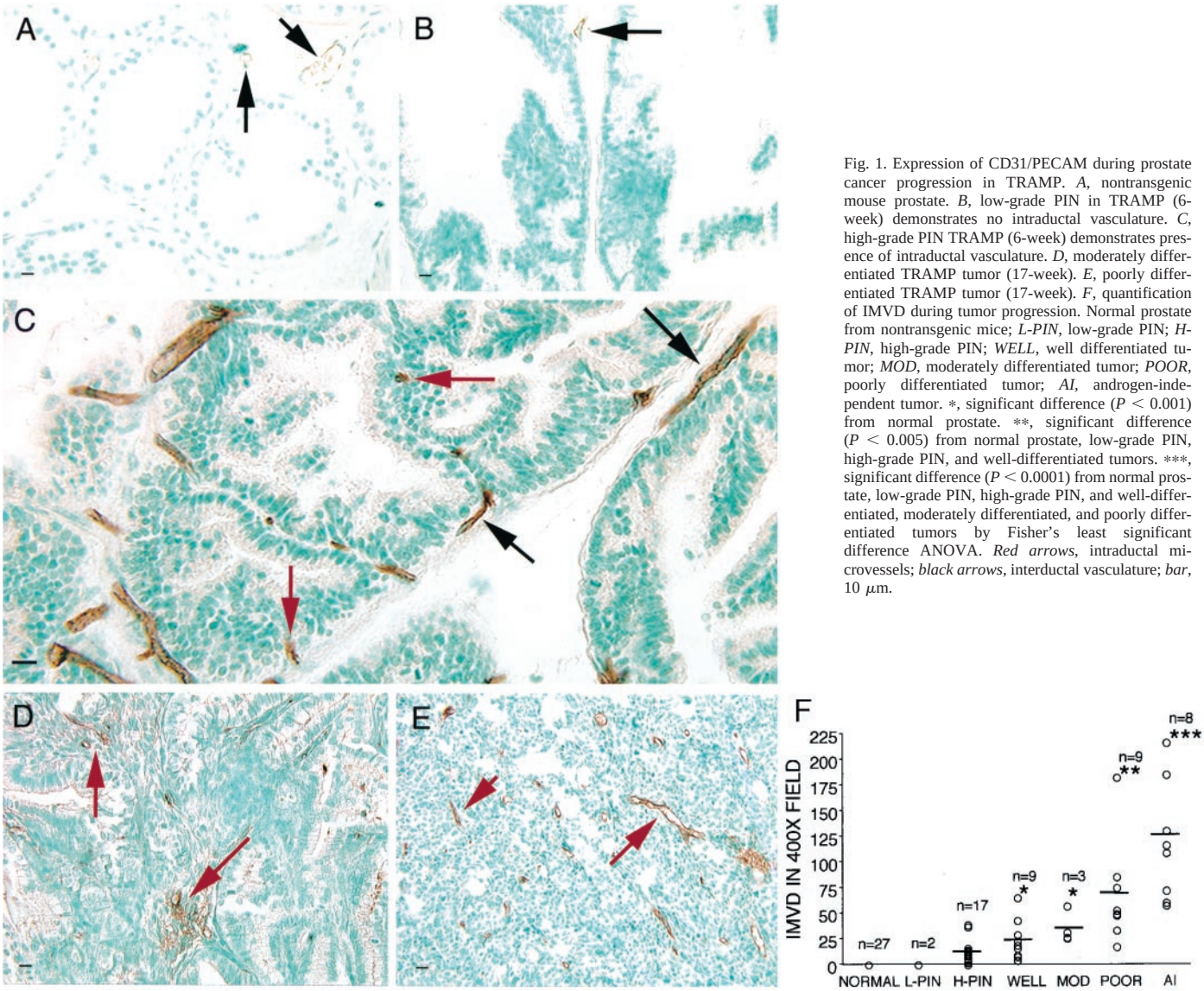

Fig. 1. Expression of CD31/PECAM during prostate cancer progression in TRAMP. *A*, nontransgenic mouse prostate. *B*, low-grade PIN in TRAMP (6-week) demonstrates no intraductal vasculature. *C*, high-grade PIN TRAMP (6-week) demonstrates presence of intraductal vasculature. *D*, moderately differentiated TRAMP tumor (17-week). *E*, poorly differentiated TRAMP tumor (17-week). *F*, quantification of IMVD during tumor progression. Normal prostate from nontransgenic mice; *L-PIN*, low-grade PIN; *H-PIN*, high-grade PIN; *WELL*, well differentiated tumor; *MOD*, moderately differentiated tumor; *POOR*, poorly differentiated tumor; *AI*, androgen-independent tumor. *, significant difference ($P < 0.001$) from normal prostate. **, significant difference ($P < 0.005$) from normal prostate, low-grade PIN, high-grade PIN, and well-differentiated tumors. ***, significant difference ($P < 0.0001$) from normal prostate, low-grade PIN, high-grade PIN, and well-differentiated, moderately differentiated, and poorly differentiated tumors by Fisher's least significant difference ANOVA. *Red arrows*, intraductal microvessels; *black arrows*, interductal vasculature; *bar*, 10 μm.

2434 of GenBank accession number L07297 (35). The VEGFR2/KDR probe (427 bp), pVEGFR2–427, was amplified with primers (forward, 5′-TTTGGAAACCTATCAACTTAC; and reverse, 5′-GGACAGGAACAAATTATCTCCAT) corresponding to bp 4085–4512 of GenBank accession number S53103 (36). All of the primers were synthesized by Genosys, Woodlands, TX, or Life Technologies, Inc., with *Sac*I and *Eco*RI or *Kpn*I and *Bam*HI sites added to the 5′-end of the forward and reverse primers, respectively. The cDNA products were directionally cloned into *Kpn*I- and *Sac*I-restricted pBluescript KS-(Stratagene, Inc.). Confirmation of the sequence and insert orientation was determined by sequence analysis (Molecular Genetics Core Facility, University of Texas-Houston Medical School). To prepare ^{33}P-probes, the plasmids were linearized with *Eco*RI or *Bam*HI restriction enzymes, and T7 or T3 polymerases were used to synthesize the antisense and sense probes, respectfully. Before hybridization, paraffin sections were hydrated in xylene and graded alcohol and equilibrated into PBS. Slides were treated with proteinase K (20 μg/ml, 15 min) and 4% paraformaldehyde (20 min) and were allowed to hybridize with RNA probes (3.5×10^6 cpm/section) at 42°C overnight in hybridization solution. Slides were washed in 2× SSC/15 mM β-mercaptoethanol (20 min), 2× SSC/RNase (40 μg/ml, 15 min), 0.1× SSC (42°C, 15 min), and 0.1× SSC (room temp, 15 min), dehydrated through graded alcohols, and dipped in Kodak NTB2 emulsion (Kodak, Rochester NY). Emulsion was developed after 5–7 days, antisense and sense of each probe were developed after equal time of emulsion, and slides were counterstained with H&E. Slides were then dehydrated through graded alcohol into xylene and mounted under glass coverslips.

RESULTS

Temporal and Spatial Pattern of PECAM-1/CD31 Expression. To elucidate the sequence of molecular events intricate with angiogenesis and the initiation and progression prostate cancer, we first examined the temporal and spatial pattern of PECAM-1/CD31 expression as a marker of vascularization in cohorts of nontransgenic and TRAMP mice. As shown in Fig. 1, vasculature was observed to be exclusively interductal in the dorsolateral prostates of nontransgenic mice at all ages (6, 12, 18, and 24 weeks). In contrast, we observed two distinct and different types of vascularization in the PIN lesions of TRAMP mice. In low-grade PIN, the vasculature was predominantly interductal (Fig. 1*B*); however, vasculature was observed to become increasingly arching the edge of the duct and progressively intraductal within epithelial clusters concomitant with the appearance of the high-grade PIN lesions (Fig. 1*C*). In the moderately and poorly differentiated TRAMP tumors, the vasculature was observed to be scattered within the tumor (Fig. 1, *D* and *E*), with the most obvious blood vessels appearing in the most poorly differentiated tumors (Fig. 1*E*). These observations demonstrate that an early angiogenic event temporally correlates with the transition between low- and high-grade PIN.

To better quantitate the vascularity of PIN lesions, the IMVD

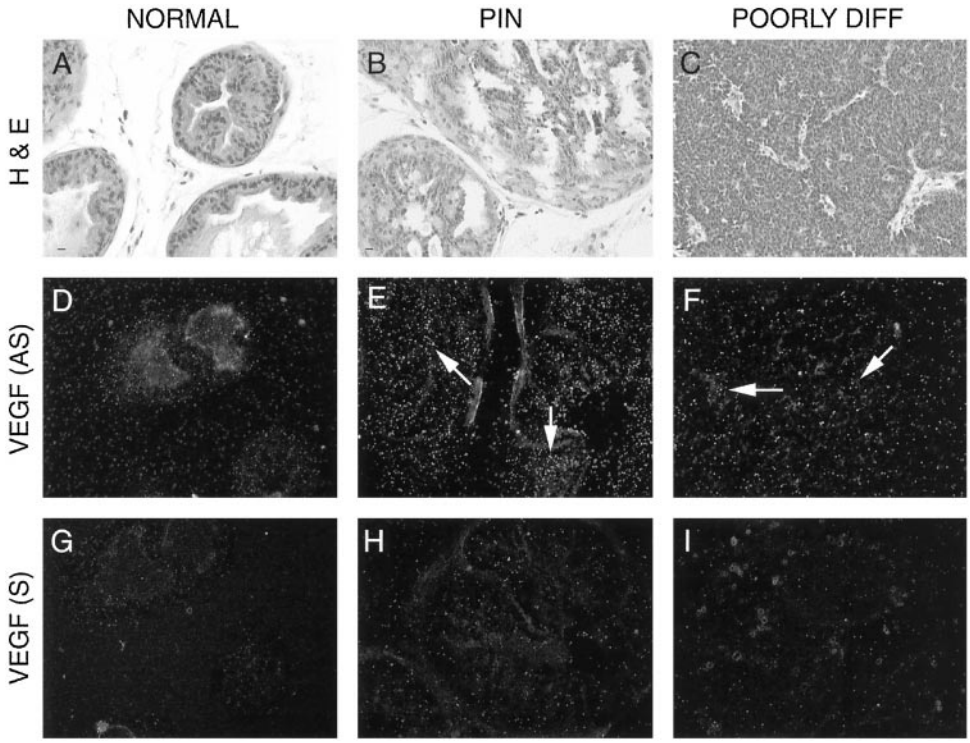

Fig. 2. Expression of VEGF during prostate tumor progression in TRAMP. Serial sections of specimens were stained H&E (*A*, *B*, and *C*). Expression of VEGF mRNA was detected in high-grade PIN of TRAMP (12-week; *E*) and poorly differentiated tumor of TRAMP (24-week; *F*). The sense control in serial sections illustrates nonspecific background (*G*, *H*, and *I*). *VEGF (AS)*, antisense VEGF probe; *VEGF (S)*, sense VEGF probe. *White arrows*, high levels of VEGF expression; *bar*, 10 μm.

was determined in three high-power fields for each sample as an index of the average number of vessels within each duct. As shown in Fig. 1*F*, intraductal microvessels were not detected in prostate samples obtained from nontransgenic mice. In contrast, only 18% (3 of 17) of high-grade PIN samples had no detectable IMVD, whereas 35% (6 of 17) of high-grade PIN samples had an IMVD between 1 and 10, and 47% (8 of 17) had an IMVD >10. When compared with nontransgenic littermates, the increase in IMVD observed in well-, moderately, and poorly differentiated and androgen-independent tumors was statistically significant ($P < 0.005$). Furthermore, the increase in IMVD was found to be a function of progression. The poorly differentiated tumors had a significant increase in IMVD when compared with low-grade PIN, high-grade PIN, and well-differentiated tumors ($P < 0.005$). In addition, the androgen-independent tumors derived from castrated mice demonstrated a significant increase in IMVD compared with all of the other stages, including the poorly differentiated tumors isolated from intact mice ($P < 0.0001$).

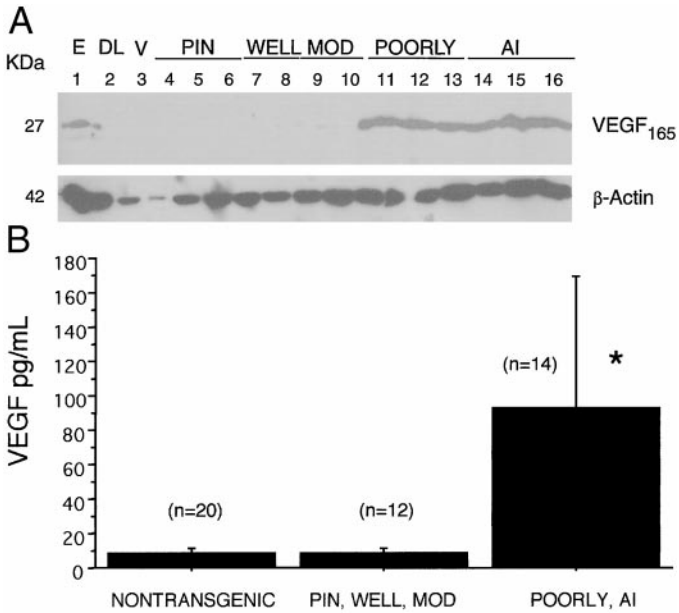

Fig. 3. Expression of VEGF in prostate and serum. *A*, expression of VEGF-165 isoform was restricted to poorly differentiated and androgen-independent tumors (*Lanes 11–16*). *KDa* (*on the left*), M_r. *B*, serum VEGF (pg/ml) was determined by immunoassay analysis. The tumor grade was determined by histology. *, significant difference ($P < 0.01$) from nontransgenic mice and mice with PIN, well, and moderately differentiated tumors.

Temporally and Spatially Restricted Expression of VEGF. To further characterize changes in the VEGF axis at the molecular level during progression of prostate cancer, *in situ* hybridization analysis was performed, in which the VEGF riboprobe was designed across the first 5 exons to detect all known isoforms of VEGF. As shown in Fig. 2, VEGF mRNA was not detected in the prostate sections obtained from nontransgenic mice (Fig. 2*D*), whereas transcripts were detected in samples representing PIN, and well- and poorly differentiated prostate cancers (Fig. 2, *E* and *F*), compared with sense riboprobe controls (Fig. 2, *G*, *H*, and *I*). In contrast, VEGF-B mRNA was readily detectable in all of the samples examined (data not shown). Transcripts encoding VEGF-C were detected in only 1 of 2 poorly differentiated tumors (data not shown).

Expression of VEGF in Prostate Correlates with Serum Levels. As shown in Fig. 3, expression of the predominant isoforms VEGF-121 and VEGF-165 were detected by immunoblotting in an extract prepared from a 12-days-post-conception mouse embryo control. However, these isoforms were not detected in the extracts prepared from dorsolateral or ventral prostate of adult mice nor in the samples prepared from PIN lesions or from well-differentiated or moderately differentiated tumors. In contrast, VEGF-165 was readily detectable in samples prepared from the poorly differentiated tumors of intact and castrated mice.

To examine possible correlations between the circulating levels of VEGF with the levels observed in prostate tissue, serum levels of VEGF-121 and VEGF-165 were determined in age-matched TRAMP

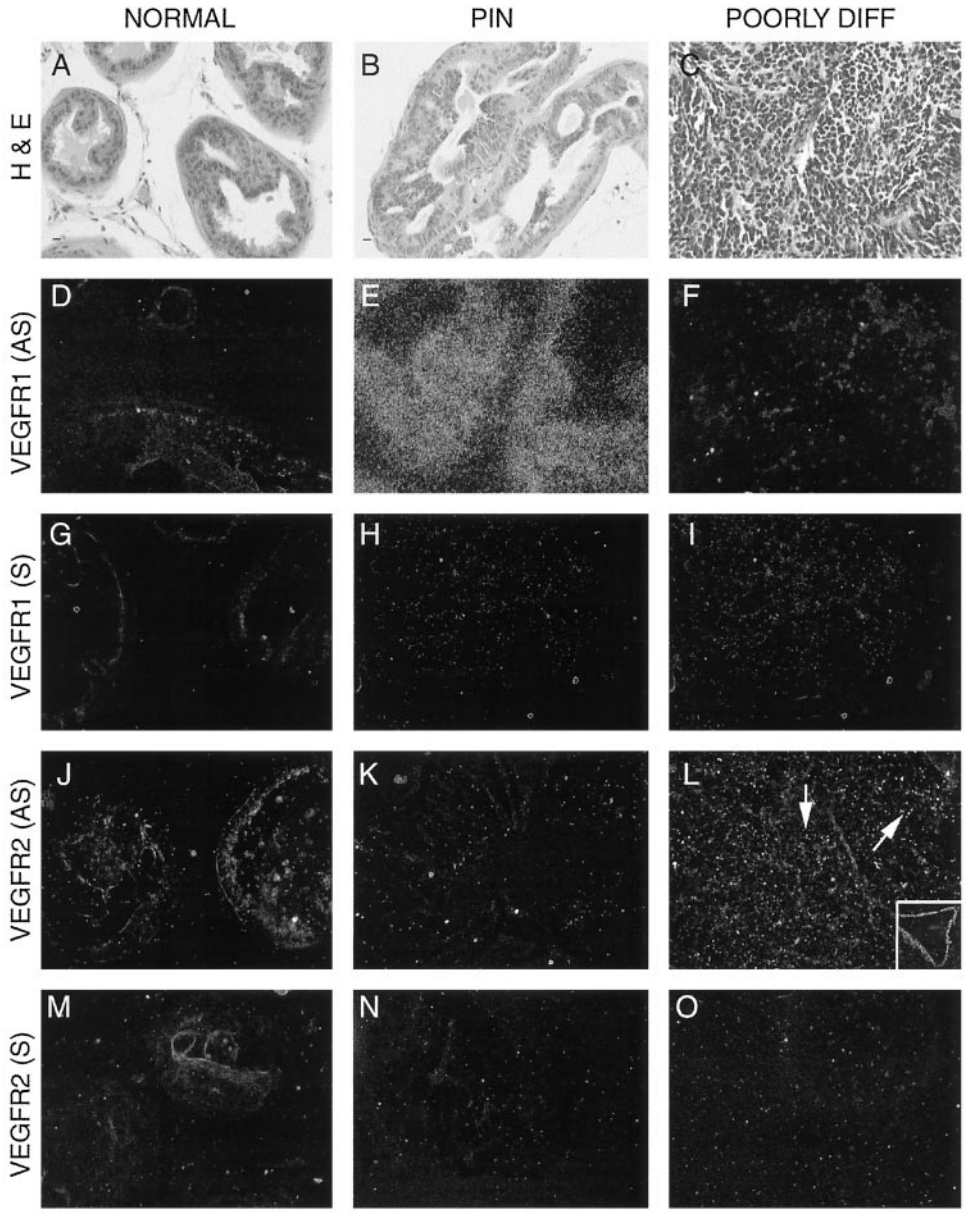

Fig. 4. Expression of VEGFR1 and VEGFR2 during prostate tumor progression in TRAMP. Serial sections of specimens were stained H&E (*A*, *B*, and *C*). VEGFR1 mRNA was observed to be expressed only in high-grade PIN (*E*). VEGFR2 mRNA was observed to be expressed only in the poorly differentiated tumor (*L*); *inset*, large vessel that expresses VEGFR2. The sense control in serial sections illustrates nonspecific background for each probe. *VEGFR1 (AS)*, antisense VEGFR1 probe; *VEGFR1 (S)*, sense VEGFR1 probe; *VEGFR2 (AS)*, antisense VEGFR2 probe; *VEGFR2 (S)*, sense VEGFR2 probe. *White arrows*, high levels of VEGFR2 expression in the vasculature. *Bar*, 10 μm.

mice and nontransgenic littermates. As shown in Fig. 3, significantly elevated levels of serum VEGF were detected in mice bearing poorly differentiated or androgen-independent tumors as compared with nontransgenic animals or animals bearing PIN or well- or moderately differentiated lesions ($P < 0.01$). There was also a strong correlation between serum VEGF levels and IMVD (F, 7.296; R^2, 0.139; $P < 0.01$), which indicated that VEGF expression is associated with a high IMVD index. It is interesting to note, that 35% (5 of 14) animals bearing a poorly differentiated or androgen-independent tumor had levels of serum VEGF between 0 and 20 pg/ml, well within the normal range. Hence, these observations also raise the possibility that other angiogenic factors, independent of VEGF, could be facilitating tumor growth in these animals.

Temporally and Spatially Restricted Expression of VEGFR1 and VEGFR2 Isoforms. Expression of VEGFR1 mRNA was detected with a riboprobe designed to recognize the alternatively spliced exon, thus making it specific for the full-length receptor, in samples representing PIN and well-differentiated tumors (Fig. 4*E*) compared with sense riboprobe controls (Fig. 4, *G*, *H*, and *I*) but not in prostate samples from nontransgenic mice (Fig. 4*D*) or in poorly differentiated tumors (Fig. 4*F*). Expression of VEGFR1 mRNA in the epithelial cells of PIN lesions and well-differentiated tumors supported our observations on the localization of VEGFR1 by immunohistochemical analysis (data not shown). Although transcripts encoding the sVEGFR1 were detected in normal prostate and samples representing PIN and well-differentiated prostate cancer, sVEGFR1 transcripts were detected in only 1 (50%) of 2 poorly differentiated tumors (data not shown). Transcripts encoding VEGFR2 were easily detected in poorly differentiated TRAMP tumors (Fig. 4*L*) compared with sense riboprobe control (Fig. 4*O*). VEGFR2 mRNA was also detectable in normal prostate (Fig. 4*J*). Hence, the *in situ* analysis demonstrates that epithelial cells in PIN lesions and in well-differentiated tumors expressed VEGFR1, whereas the majority of VEGFR2 expression appears to be restricted to endothelial cells that are representative of more advanced prostate cancer.

Expression of VEGFR1 and VEGFR2 Isoforms Are Associated with Prostate Cancer Progression. Using immunoblot analysis, we found VEGFR1 expression to be predominate in the samples representing PIN lesions and well- and moderately differentiated tumors (Fig. 5) in general agreement with our *in situ* analysis. It is

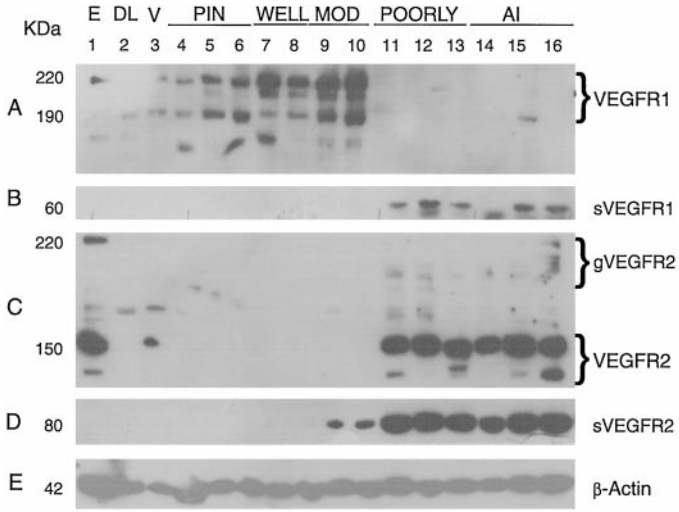

Fig. 5. VEGF receptor isoforms during tumor progression in TRAMP. *E*, 12-day embryo; *DL*, normal dorsolateral prostate; *V*, normal ventral prostate. In *A*, expression of VEGFR1 was restricted to normal dorsolateral and ventral prostate (*Lanes 2–3*), *PIN* (*Lanes 4–6*), well-differentiated tumors (*Lanes 7* and *8*), and moderately differentiated tumors (*Lanes 9* and *10*). In *B*, expression of sVEGFR1 was restricted to poorly differentiated and androgen-independent tumors (*Lanes 11–16*). In *C*, expression of glycosolated VEGFR2 (*gVEGFR2*) and VEGFR2 was restricted to poorly differentiated and androgen-independent tumors (*Lanes 11–16*). In *D*, expression of short VEGFR2 (sVEGFR2) was restricted to moderately differentiated (*Lanes 9* and *10*) and poorly differentiated and androgen-independent tumors (*Lanes 11–16*). In *E*, expression of β-actin was used as a loading control. *PIN*, high-grade PIN; *WELL*, well-differentiated tumors; *MOD*, moderately differentiated tumors; *POORLY*, poorly differentiated tumors; *AI*, androgen-independent tumors.

interesting to note that the sVEGFR1 was detected only in the high-grade tumors (Fig. 5*B*). Similarly, expression of VEGFR2 was primarily detectable in the high-grade tumors (Fig. 5*C*). Although expression of VEGFR2 was also detectable in normal prostate, it was surprising to note that VEGFR2 expression was not detectable in PIN or in well-differentiated or moderately differentiated lesions (Fig. 5*C*). The expression of the short form of VEGFR2 (sVEGFR2) was readily detectable in moderately, poorly differentiated, and androgen-independent tumors (Fig. 5*D*). On the basis of this analysis, there appears to be a profound and invariant switch between the expression of VEGFR1 and VEGFR2 during the progression of prostate cancer that correlates with the transition from a differentiated to a poorly differentiated disease.

HIF-1α Expression Is an Early Angiogenic Event in Prostate Cancer. The transcription factor HIF-1α has been shown previously to regulate the expression of VEGF and VEGFR1. Hence, we examined the expression of HIF-1α during the progression of prostate cancer in the TRAMP model. As shown in Fig. 6, HIF-1α was detected by immunohistochemistry in PIN lesions and in well-differentiated and poorly differentiated tumors (Fig. 6, *B*, *C*, and *D*) but not in the prostate glands of nontransgenic mice (Fig. 6*A*). It is interesting to note that the samples representative of PIN lesions with the highest level of VEGF and VEGFR1 mRNA expression also expressed substantial levels of HIF-1α in the nucleus (Fig. 6*B*). Therefore, it appears that expression of HIF-1α correlates with, and perhaps precedes, the expression of VEGFR1 and VEGF mRNA in PIN lesions.

The VEGF Axis in Clinical Prostate Cancer. Using TRAMP as a predictive model for clinical disease, the expression of VEGF and the VEGFRs was examined in 30 samples obtained from the S.P.O.R.E. prostate tissue bank at Baylor College of Medicine. The clinical specimens represented Gleason grades 5–7, and normal sections from each patient were used as controls. Protein extracts were prepared from normal and prostate cancer samples and then assayed by immunoblotting for VEGF, VEGFR1, and VEGFR2. As shown in Table 1, there were no significant changes observed in the level of VEGF expression in the cancer samples [21 (70%) of 30] when compared with the normal samples [19 (63%) of 30]. However there was a significant decrease in VEGFR1 expression in the cancer samples [21 (70%) of 30] when compared with the normal samples [28 (93%) of 30; $P < 0.05$]. Even more striking was the increase in VEGFR2 expression in the cancer samples [25 (83%) of 30] when compared with the normal samples [11 (37%) of 30; $P < 0.0001$). It is also interesting to note that 8 (27%) of 30 of this collection of similarly matched cancer samples lost VEGFR1 expression whereas 15 (50%) of 30 gained VEGFR2 expression when compared with the matched normal samples. This analysis of human prostate specimens not only validates the predictive nature of the TRAMP model but also validates VEGF

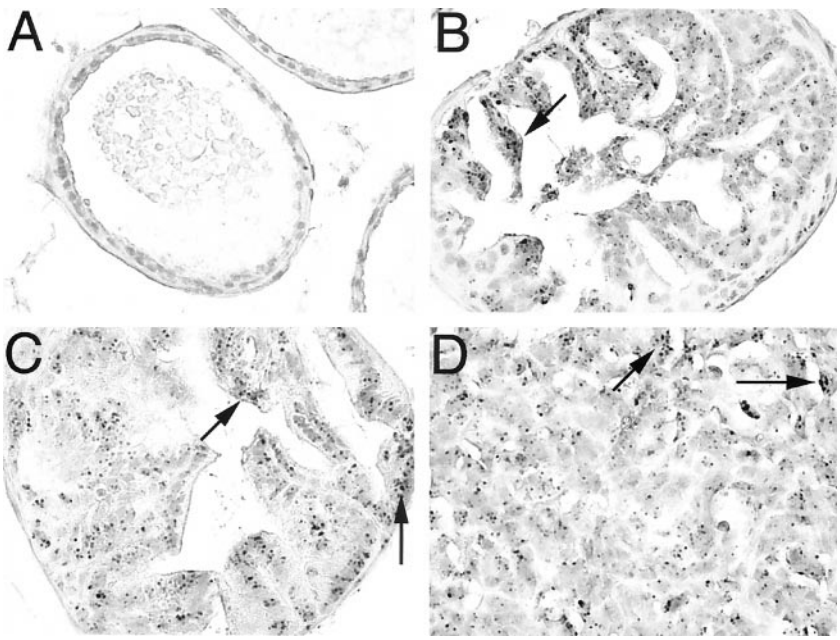

Fig. 6. HIF-1α expression in TRAMP. *A*, normal mouse prostate. *B*, high-grade PIN of TRAMP (12-week). *C*, well-differentiated tumor of TRAMP (18-week). *D*, poorly differentiated tumor of TRAMP (24-week). Expression of HIF-1α was detected in PIN and in well- and poorly differentiated tumors. *Black arrows*, high expression of HIF-1α in the nuclei of epithelial and tumor cells. $\times$400.

Table 1 *Expression of VEGF, VEGFR1, and VEGFR2 in human and TRAMP prostate cancer*

	VEGF	VEGFR1	VEGFR2
Human			
Normal	19/30 (63%)	28/30 (93%)	11/30 (37%)
Cancer	21/30 (70%)	21/30 (70%)[a]	25/30 (83%)[b]
TRAMP			
Non-transgenic	0/4 (0%)	4/4 (100%)	1/4 (25%)
PIN,[c] WDA, MDA	0/9 (0%)	7/7 (100%)	0/7 (0%)
PDA, AIA	6/6 (100%)[d]	1/7 (14%)[e]	7/7 (100%)[e]

[a] Significantly different than normal ($P < 0.05$).
[b] Significantly different from normal ($P < 0.0001$).
[c] PIN, high-grade PIN; WDA, well-differentiated adenocarcinoma; MDA, moderately differentiated adenocarcinoma; PDA, poorly differentiated adenocarcinoma; AIA, androgen-independent adenocarcinoma.
[d] Different from nontransgenic, PIN, WDA, and MDA.
[e] Significantly different from nontransgenic, PIN, WDA, and MDA ($P < 0.001$).

receptor switching as a molecular marker of prostate cancer progression.

DISCUSSION

It has been difficult to identify and characterize the earliest molecular changes that facilitate angiogenesis in clinical prostate cancer mostly because of the limited availability and access to human tissue representing early-stage disease. A number of studies have demonstrated that human prostate tumors and cell lines can express VEGF; however, VEGF has also been detected in normal prostate and BPH, which reveals the difficulty inherent in a comprehensive analysis of human prostate cancer specimens. For example, in one study, the level of VEGF mRNA was found to be overexpressed 3-fold or more in 29% of prostate cancer when compared with normal prostate (37). In another study, VEGF protein was detected in 90% of prostate cancers and 100% of BPH specimens (9). However, in a separate study, VEGF protein was detected in 80% of prostate cancer, 18% of BPH, and 0% normal prostate samples (8). Clearly there is some degree of controversy regarding the relationship between VEGF expression and prostate disease, complicated by the fact that prostate cancer is a heterogeneous disease of a heterogeneous population. Therefore, the goal of this study was to specifically examine expression of the VEGF axis at the molecular level during the progression prostate cancer in a spontaneous inbred autochthonous model that closely mimics the natural history of human prostate cancer.

On the basis of our observations, we propose that there are, in fact, two angiogenic events consistent with the progression of TRAMP and clinical prostate cancer. As shown in Fig. 7, the early angiogenic "initiation switch" correlates expression of HIF1-α and VEGFR1 in addition to the recruitment and elaboration of intraductal vasculature in PIN lesions. Because HIF-1α has previously been shown to initiate the transcription of VEGF and VEGFR1 mRNA (16, 17), it was not surprising to note that these transcripts were also found to be expressed in PIN. Hence, these observations are consistent with previous reports showing HIF-1α to be expressed in preneoplastic lesions and in human prostate cancer (29).

Although the expression of VEGF mRNA was observed to be elevated in PIN lesions and well-differentiated tumors, we were unable to detect or localize VEGF protein in these samples. This suggests that the level of VEGF protein was below the limit of sensitivity of our assay or that posttranscriptional regulation of VEGF may be operational in these lesions. In fact, expression of HIF-1α is indicative of a hypoxic response and hypoxia has been shown to induce translation of VEGF mRNA through a 5′-untranslated region internal ribosome entry site (38, 39). This indicates that VEGF expression in prostate cancer under hypoxic conditions may be regulated through mechanisms including, but not limited to, transcription, mRNA stability, and translation. Elucidation of the nature of this regulation will require additional studies at the molecular level. In contrast, VEGFR1 mRNA and protein were both readily observed in the endothelial and tumor epithelial cells in low-grade tumors. Although VEGFR1 has generally been considered to be endothelial cell-specific, there are a number of recent reports of VEGFR1 expression in mammary carcinomas, glioblastomas, squamous cell carcinoma of the head and neck, and prostate carcinomas (40–42).

In addition to the early initiation switch, our data also provide evidence for a later progression switch consistent with the high level expression of VEGF protein in the prostatic tissues and serum of TRAMP mice harboring advanced, poorly differentiated, and androgen-independent tumors. This observation also suggests that the prostate is a source of VEGF and that tumor growth is at least partially dependent on this expression. Furthermore, our data suggest that prostatic VEGF likely is secreted only after the tumor is no longer organ confined. The correlation between serum VEGF, IMVD, and the transition of a differentiated tumor to a poorly differentiated tumor also supports a causal relationship between serum VEGF and tumor progression.

Consistent with the progression switch is the observation that expression of VEGFR2 in the vasculature is concomitant with the loss of VEGFR1 and an increase in IMVD in poorly differentiated high-grade tumors (Fig. 7). This is consistent with the functions ascribed to these receptors. Although VEGFR1 is important in endothelial cell migration, the receptor does not appear to signal through MAPK nor induce endothelial cell proliferation (23). In contrast, VEGFR2 has been demonstrated to signal through MAPK to induce endothelial cell proliferation and through PI3′K imparting an antiapoptotic function in

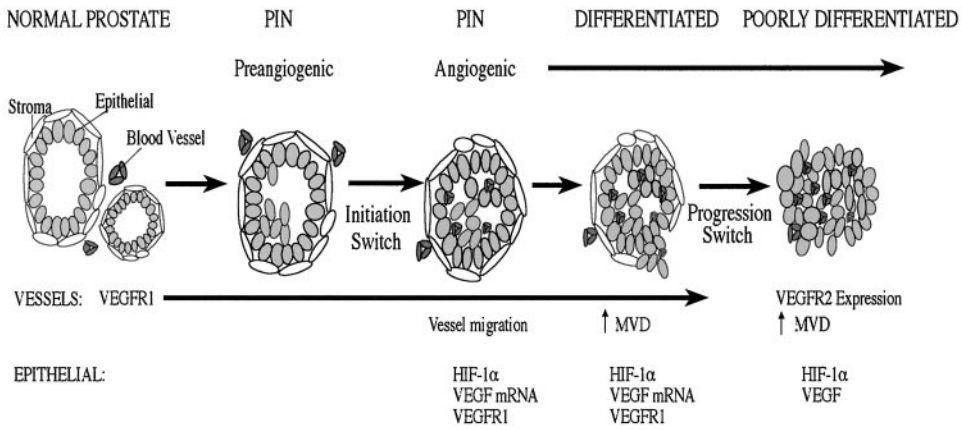

Fig. 7. Schematic representation of the angiogenic switch in TRAMP. Normal prostate has prominent interductal vasculature, with VEGFR1 expression. Preangiogenic PIN lesions express VEGFR1 and demonstrate a hypoxic environment that can stabilize HIF-1α. At this stage, the vasculature is interductal. Concomitant with PIN there is an angiogenic initiation switch that correlates with noticeable vessel migration into the prostatic duct, and the epithelial cells express HIF-1α. VEGF mRNA is expressed by the tumor cells and VEGFR1 mRNA and protein are expressed by the tumor and endothelial cells. A second-event angiogenic progression switch is consistent with progression to a poorly differentiated tumor. In the poorly differentiated tumors, endothelial cells express VEGFR2 and HIF-1α, and a detectable level of VEGF is expressed by tumor cells.

endothelial cells (24, 25). Hence, the molecular changes observed in clinical and TRAMP prostate cancer progression relate to the specific biochemical properties of the various components of the VEGF axis and demonstrate that these components, in fact, represent specific therapeutic targets.

The similar trends observed in the temporal pattern of VEGFR expression in the clinical and TRAMP specimens validate the predictive nature of such mouse models of human cancer. Although the VEGF receptor switch was not as clearly defined in the clinical samples, these studies underscore how difficult it is to resolve the heterogeneity inherent in clinical disease. Nevertheless, to our knowledge this is the first report demonstrating an angiogenic initiation switch that correlates with PIN in prostate cancer in an animal model. Furthermore, we have also demonstrated that a second progression switch is a function of the differential expression of VEGFR1 and VEGFR2. Studies are currently underway to determine whether therapies designed to target these specific molecules will prove efficacious in a preclinical trail. Lastly, we have demonstrated that the data obtained with the mouse model can indeed be predicative of the molecular events operating in human disease.

ACKNOWLEDGMENTS

We thank Drs. Paula Kaplan and Barbara Foster for thoughtful discussions, Drs. Michael Ittmann and David Rowely for critical reading of the manuscript, Drs. Gregg Semenza and Hua Zhong for help with the HIF-1α staining, Caroline Castile and Rhonda Chaplin for support with animal husbandry, and Alvenia Daniels for secretarial support.

REFERENCES

1. Gimbrone, M. A. J., Leapman, S. B., Cotran, R. S., and Folkman, J. Tumor dormancy *in vivo* by prevention of neovascularization. J. Exp. Med., *136:* 261–276, 1972.
2. Hanahan, D., and Folkman, J. Patterns and emerging mechanisms of the angiogenic switch during tumorigenesis. Cell, *86:* 353–364, 1996.
3. Zetter, B. R. Angiogenesis and tumor metastasis, Annu. Rev. Med., *49:* 407–424, 1998.
4. Leung, D. W., Cachianes, G., Kuang, W-J., Goeddel, D. V., and Ferrara, N. Vascular endothelial growth factor is a secreted angiogenic mitogen. Science (Washington DC)., *246:* 1306–1309, 1989.
5. Olofsson, B., Pajusola, K., Kaipainen, A., von Euler, G., Joukov, V., Saksela, O., Orpana, A., Pettersson, R. F., Alitalo, K., and Eriksson, U. Vascular endothelial growth factor B, a novel growth factor for endothelial cells. Proc. Natl. Acad. Sci. USA, *93:* 2576–2581, 1996.
6. Joukov, V., Pajusola, K., Kaipainen, A., Chilov, D., Lahtinen, I., Kukk, E., Saksela, O., Kalkkinen, N., and Alitalo, K. A novel vascular endothelial growth factor, VEGF-C, is a ligand for the Flt4 (VEGFR-3) and KDR (VEGFR-2) receptor tyrosine kinases. EMBO J., *15:* 290–298, 1996.
7. Salven, P., Lymboussaki, A., Heikkila, P., Jaaskela-Saari, H., Enholm, B., Aase, K., von Euler, G., Eriksson, U., Alitalo, K., and Joensuu, H. Vascular endothelial growth factors VEGF-B and VEGF-C are expressed in human tumors. Am. J. Pathol., *153:* 103–108, 1998.
8. Ferrer, F. A., Miller, L. J., R. I., A., Kurtzman, S. H., Albertsen, P. C., Laudone, V. P., and Kreutzer, D. L. Vascular endothelial growth factor (VEGF) expression in human prostate cancer: *in situ* and *in vitro* expression of VEGF by human prostate cancer cells. J. Urol., *157:* 2329–2333, 1997.
9. Jackson, M. W., Bentel, J. M., and Tilley, W. D. Vascular endothelial growth factor (VEGF) expression in prostate cancer and benign prostatic hyperplasia. J. Urol., *157:* 2323–2328, 1997.
10. Ferrer, F. A., Miller, L. J., Andrawis, R. I., Kurtzman, S. H., Albertsen, P. C., Laudone, V. P., and Kreutzer, D. L. Angiogenesis and prostate cancer. *In vivo* and *in vitro* expression of angiogenesis factors by prostate cancer cells. Urology, *51:* 161–167, 1998.
11. Weingartner, K., Ben-Sasson, S. A., Stewart, R., Richie, J. P., Riedmeiller, H., and Folkman, J. Endothelial cell proliferation activity in benign prostatic hyperplasia and prostate cancer: an *in vitro* model for assessment. J. Urol., *159:* 465–470, 1998.
12. Haggstrom, S., Wikstrom, P., Bergh, A., and Damber, J. E. Expression of vascular endothelial growth factor and its receptors in the rat ventral prostate and Dunning R3327 PAP adenocarcinoma before and after castration. Prostate, *36:* 71–79, 1998.
13. Connolly, J. M., and Rose, D. P. Angiogenesis in two human prostate cancer cell lines with differing metastatic potential when growing as solid tumors in nude mice. J. Urol., *160:* 932–936, 1998.
14. Marti, H. H., and Risau, W. Systemic hypoxia changes the organ-specific distribution of vascular endothelial growth factor and its receptors. Proc. Natl. Acad. Sci. USA, *95:* 15809–15814, 1998.
15. Levy, A. P., Levy, N. S., and Goldberg, M. A. Post-transcriptional regulation of vascular endothelial growth factor by hypoxia. J. Biol. Chem., *271:* 2746–2753, 1996.
16. Forsythe, J. A., Jiang, B-H., Iyer, N. V., Agani, F., Leung, S. W., Koos, R. D., and Semenza, G. L. Activation of vascular endothelial growth factor gene transcription by hypoxia-inducible factor 1. Mol. Cell. Biol., *16:* 4604–4613, 1996.
17. Gerber, H. P., Condorelli, F., Park, J., and Ferrara, N. Differential transcriptional regulation of the two vascular endothelial growth factor receptor genes. J. Biol. Chem., *272:* 23659–23667, 1997.
18. Kappel, A., Volker, R., Damert, A., Lamme, I., Pisau, W., and Breier, G. Identification of vascular endothelial growth factor (VEGF) receptor-2 (Flk-1) promoter/enhancer sequences sufficient for angioblast and endothelial cell-specific transcription in transgenic mice. Blood, *93:* 4284–4292, 1999.
19. Seghezzi, G., Sundeep, P., Ren, C. J., Gualandris, A., Pintucci, G., Robbins, E. S., Shapiro, R. L., Galloway, A. C., Rifkin, D. B., and Mignatti, P. Fibroblast growth factor-2 (FGF-2) induces vascular endothelial growth factor (VEGF) expression in the endothelial cells of forming capillaries: an autocrine mechanism contributing to angiogenesis. J. Cell Biol., *141:* 1659–1673, 1998.
20. Warren, R. S., Yuan, H., Matli, M. R., Ferrara, N., and Donner, D. B. Induction of vascular endothelial growth factor by insulin-like growth factor 1 in colorectal carcinoma. J. Biol. Chem., *271:* 29483–29488, 1996.
21. Levine, A. C., Liu, X., Greenberg, P. D., Eliashvili, M., Schiff, J. D., Aaronson, S. A., Holland, J. F., and Kirschenbaum, A. Androgens induce the expression of vascular endothelial Growth factor in human fetal prostatic fibroblasts. Endocrinology, *139:* 4672–4678, 1998.
22. Ito, N., Wernstedt, C., Engstrom, U., and Claesson-Welsh, L. Identification of vascular endothelial growth factor receptor-1 tyrosine phosphorylation sites and binding of SH2 domain-containing molecules. J. Biol Chem., *273:* 23410–23418, 1998.
23. Waltenberger, J., Claessonwelsh, L., Siegbahn, A., Shibuya, M., and Heldin, C. H. Different signal transduction properties of KDR and Flt-1. Two receptors for vascular endothelial growth factor. J. Biol. Chem., *269:* 26988–26995, 1994.
24. Kroll, J., and Waltenberger, J. The vascular endothelial growth factor receptor KDR activates multiple signal transduction pathways in porcine aortic endothelial cells. J. Biol. Chem., *272:* 32531–32527, 1997.
25. Gerber, H. P., McMurtrey, A., Kowalski, J., Yan, M., Keyt, B. A., Dixit, V., and Ferrara, N. Vascular endothelial growth factor regulates endothelial cell survival through the phosphatidylinositol 3′-kinase/Akt signal transduction pathway. J. Biol. Chem., *273:* 30336–30343, 1998.
26. Greenberg, N. M., DeMayo, F., Finegold, M. J., Medina, D., Tilley, W. D., Aspinall, J. O., Cunha, G. R., Donjacour, A. A., Matusik, R. J., and Rosen, J. M. Prostate cancer in a transgenic mouse. Proc. Natl. Acad. Sci. USA, *92:* 3439–3443, 1995.
27. Gingrich, J. R., and Greenberg, N. M. A transgenic mouse prostate cancer model. Toxicol. Path., *24:* 502–504, 1996.
28. Gingrich, J. R., Barrios, R. J., Foster, B. A., and Greenberg, N. M. Pathologic progression of autochthonous prostate cancer in the TRAMP model. Prostate Cancer Prostatic Dis., *6:* 1–6, 1999.
29. Zhong, H., De Marzo, A. M., Laughner, E., Lim, M., Hilton, D. A., Zagzag, D., Buechler, P., Isaacs, W. B., Semenza, G. L., and Simons, J. W. Overexpression of hypoxia-inducible factor 1α in common human cancers and their metastases. Cancer Res., *59:* 5830–5835, 1999.
30. Kawasaki, E. S. Amplification of RNA. *In:* M. A. Innis, D. H. Gelfand, J. J. Snisky, and T. J. White (eds.), PCR Protocols: A Guide to Methods and Applications, pp. 21–27. New York: Academic Press, 1990.
31. Claffey, K. P., Wilkison, W. O., and Spiegelman, B. M. Vascular endothelial growth factor: regulation by cell differentiation and activated second messenger pathways. J. Biol. Chem., *267:* 16317–16322, 1992.
32. Townson, S., Lagercrantz, J., Grimmond, S., and Silins, G. Characterization of the murine VEGF-related factor gene. Biochem. Biophys. Res. Commun., *220:* 922–928, 1996.
33. Kukk, E., Lymboussaki, A., Taira, S., Kaipainene, A., Jeltsch, M., Joukov, V., and Alitalo, K. VEGF-C receptor binding and pattern of expression with VEGFR-3 suggests a role in lymphatic vascular development. Development (Camb.), *122:* 3829–3837, 1996.
34. Kendall, R. L., and Thomas, K. A. Inhibition of vascular endothelial cell growth factor activity by an endogenously encoded soluble receptor. Proc. Natl. Acad. Sci., *90:* 10705–10709, 1993.
35. Finnerty, H., Kelleher, K., Morris, G. E., Bean, K., Merberg, D. M., Kriz, R., Morris, J. C., Sookdeo, H., Turner, K. J., and Wood, C. R. Molecular cloning of murine FLT and FLT4. Oncogene., *8:* 2293–2298, 1993.
36. Oelrichs, R. B., Reid, H. H., Bernard, O., Ziemiecki, A., and Wilks, A. F. NYK/FLK-1: a putative receptor protein tyrosine kinase isolated from E10 embryonic neuroepithelium is expressed in endothelial cells of the developing embryo. Oncogene., *8:* 11–18, 1993.
37. Latil, A., Bieche, I., Pesche, S., Valeri, A., Fournier, G., Cussenot, O., and Lidereau, R. VEGF overexpression in clinically localized prostate tumors and neuropilin-1 overexpression in metastatic forms. Int. J. Cancer, *89:* 167–171, 2000.
38. Akiri, G., Nahari, D., Finkelstein, Y., Le, S. Y., Elroy-Stein, O., and Levi, B. Z. Regulation of vascular endothelial growth factor (VEGF) expression is mediated by internal initiation of translation and alternative initiation of transcription. Oncogene, *17:* 227–236, 1998.
39. Stein, I., Itin, A., Einat, P., Skaliter, R., Grossman, Z., and Keshet, E. Translation of vascular endothelial growth factor mRNA by internal ribosome entry: implications for translation under hypoxia. Mol. Cell. Biol., *18:* 3112–3119, 1998.
40. Xie, B., Tam, N. N., Tsao, S. W., and Wong, Y. C. Co-expression of vascular endothelial growth factor (VEGF) and its receptors (flk-1 and flt-1) in hormone-induced mammary cancer in the noble rat. Br. J. Cancer, *8:* 1335–1343, 1999.
41. Herold-Mende, C., Steiner, H. H., Andl, T., Riede, D., Buttler, A., Reisser, C., Fusenig, N. E., and Mueller, M. M. Expression and functional significance of vascular endothelial growth factor receptors in human tumor cells. Lab. Investig. *79:* 1573–1582, 1999.
42. Ferrer, F. A., Miller, L. J., Lindquist, R., Kowalczyk, P., Laudone, V. P., Albertsen, P. C., and Kreutzer, D. L. Expression of vascular endothelial growth factor receptors in human prostate cancer. Urology, *54:* 567–572, 1999.

Angiogenesis and Prostate Cancer: Identification of A Molecular Progression Switch

Wendy J. Huss, Colleen F. Hanrahan, Roberto J. Barrios, et al.

Cancer Res 2001;61:2736-2743.